JOURNAL OF CATALYSIS 112, 183–193 (1988)

Effect of NO on the CO-Induced Disruption of Rhodium Crystallites

FRIGYES SOLYMOSI, TAMÁS BÁNSÁGI, AND ÉVA NOVÁK

Reaction Kinetics Research Group of the Hungarian Academy of Sciences and Institute of Solid State and Radiochemistry, University of Szeged, P.O. Box 105, H-6701 Szeged, Hungary

Received November 23, 1987; revised February 8, 1988

The effect of NO on the CO-induced oxidative disruption and reductive agglomeration of alumina-supported Rh has been investigated by means of infrared spectroscopy. On addition of NO to CO the development of gem-dicarbonyl, $Rh^I(CO)_2$, from Rh_x–CO species, indicative of the occurrence of the oxidative disintegration of Rh_x cluster, is greatly accelerated. Even a small amount of NO (NO/CO ratio = 1/100) led to a readily observable effect. It is suggested that NO forming strong bonds with Rh_x crystallites also causes the oxidative disruption of Rh–Rh bonds and gives rise to the formation of Rh^I sites. This effect was exhibited by spectral changes observed following NO adsorption on high-temperature reduced Rh_x crystallites. On the other hand, in the presence of NO the transformation of the gem-dicarbonyl into Rh_x–CO induced by CO above 448 K is significantly slowed, which means that the reductive agglomeration of Rh^I sites is hindered by NO.

INTRODUCTION

The interaction of CO with supported Rh has been the subject of extensive research in the past decade. Several surface species have been identified by infrared spectroscopy (*1*, *2*), the dominant ones being $Rh(CO)_2$, Rh–CO, and Rh_2CO. The most unusual and controversial surface species is undoubtedly gem-dicarbonyl. In contrast with the earlier belief that this forms on isolated Rh atoms (*3*, *4*) or on Rh rafts (*5*), data accumulating in recent years strongly support the view (*6*, *7*) that gem-dicarbonyl is bonded to Rh^I sites (*2*). Recent EXAFS measurements (*8–10*) showed that even Rh reduced at 593 K under flowing hydrogen is in the form of crystallites consisting of 15–20 rhodium atoms, and the formation of isolated Rh^I sites requires the presence of CO.

Recently, Solymosi and Pásztor (*11*) demonstrated that the effect of CO on the topology of Rh is twofold. At 300–400 K it leads to the oxidative disruption of Rh–Rh bonds and the formation of gem-dicarbonyl. Above 423 K, however, the presence of CO results in the reductive agglomeration of Rh^I and in the formation of linearly bonded CO at the expense of gem-dicarbonyl.

As regards the oxidation of rhodium, we favor the view that the reduction of OH groups on the support is responsible for Rh^I formation (*11*), as first proposed by Smith *et al.* (*12*) for the transformation of $Rh_6(CO)_6$ clusters supported on alumina. The findings of Solymosi and Pásztor (*11*) that the oxidative disruption of Rh_x occurs only slowly under dry conditions, and that traces of water significantly accelerate the process, provided experimental evidence for this assumption. This idea is in contrast with the belief that Rh^I is formed via the dissociation of CO (*6*, *9*, *10*, *13*). The detailed study by Solymosi and Erdöhelyi (*14*, *15*) demonstrated that the dissociation of CO over supported Rh (alumina, magnesia, silica, and titania were used as supports) occurs only above 473 K. On the other hand, the formation of gem-dicarbonyl was observed far below room temperature (*6*, *16*), where the dissociation of CO can be completely excluded. A recent study (*17*), demonstrating that isolated OH groups on the support are consumed as CO interacts

0021-9517/88 $3.00

with Rh crystallites, provides further evidence for the view that OH groups are involved in the oxidation process.

As regards the effects of other gases, it has been shown (*18*) that the presence of hydrogen inhibits the oxidative disruption, but greatly accelerates the reductive agglomerization. Similar observations were made by Zaki *et al.* (*16*). This effect of hydrogen and the formation of rhodium carbonyl hydride, $Rh\begin{matrix}CO\\H\end{matrix}$, were considered to be the main reason why the adsorbed CO formed in surface reactions on highly dispersed Rh did not lead to the disruption of the Rh–Rh bonds, i.e., to the formation of gem-dicarbonyl (*18, 19*).

In the present study we examine the surface interaction of NO and CO on highly and less dispersed Rh deposited on an Al_2O_3 support. The primary aim of the study is to establish how NO adsorbed on Rh influences the CO-induced oxidative disruption and reductive agglomerization of Rh.

The coadsorption of NO and CO on Rh/Al_2O_3 has been investigated in great detail by Arai and Tominaga (*20*) and Solymosi and Sárkány (*21*). The most interesting feature of the interaction is the formation of the $Rh\begin{matrix}CO\\NO\end{matrix}$ species at lower temperatures, 300–400 K, and the production of an isocyanate species, absorbing at 2260 cm^{-1}, at higher temperatures (*20–22*).

As regards the location of the NCO species, our laboratory presented strong evidence that, in contrast with earlier views (*22, 23*), it is situated not on the metal, but exclusively on the support (*21, 24–26*). This has been corroborated by recent findings (*27, 28–30*).

EXPERIMENTAL

IR spectra were recorded with a Specord 75 IR double-beam spectrometer (Zeiss, Jena) with a wavenumber accuracy of ±5 cm^{-1}. Two different cells were used. In the high-temperature cell the spectra were taken at the adsorption temperature. In a Kiselev-type IR cell, all spectra were recorded at the temperature of the infrared beam, ~313 K. The cells were connected to a vacuum line and to a closed circulation system in which the gases were circulated during adsorption by a small magnetic pump.

Rh/Al_2O_3 samples were prepared by incipient wetting of Al_2O_3 (Degussa, BET area 100 m^2/g) with an aqueous solution of $RhCl_3$. After impregnation, the samples were dried in air at 373 K.

For the IR studies, the dried Rh/Al_2O_3 powder was pressed into thin self-supporting wafers (30 × 10 mm, 20 mg/cm^2). The pretreatment of the samples was performed in the vacuum IR cell: the samples were (a) heated (20 K min^{-1}) to 573 K under constant evacuation, (b) oxidized with 100 Torr O_2 (1 Torr = 133.3 Pa) for 60 min at 573 K, (c) evacuated for 30 min, and (d) reduced with 100 Torr H_2 for 60 min at 573–1273 K. This was followed by degassing at the same temperature for 30 min and by cooling the sample to the temperature of the experiment. The gases were circulated during the oxidation and reduction processes. Data for the adsorption of H_2 on reduced samples are shown in Table 1. R_T signifies reduction temperature.

The gases used were of commercial purity. CO (99.9%) was purified by bubbling through a $Mn(OH)_2$ suspension. Water va-

TABLE 1

Adsorption of H_2 on 2% Rh/Al_2O_3 at 300 K

Reduction temperature (K)	H/Rh
573	0.40
673	0.34
873	0.20
1023	0.15
1273	0.07

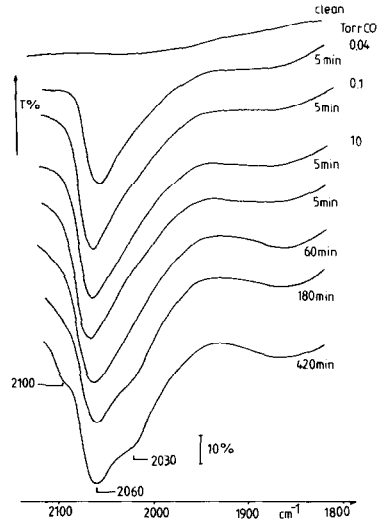

FIG. 1. Changes in the IR spectrum of 2% Rh/Al_2O_3 (R_T = 1273 K) in the presence of CO at 300 K as a function of adsorption time.

por was frozen out by a trap cooled with a dry ice–acetone mixture.

RESULTS

1. CO Adsorption

We observed in our previous work that the oxidative disruption of highly dispersed Rh crystallites (R_T = 573–673 K) is immeasurably fast at 300 K, but the process can be slowed down drastically and can be conveniently followed after high-temperature reduction (R_T = 1173–1273 K) of the rhodium sample. In this case, as shown in Fig. 1, the adsorption of CO initially produces a strong band at 2060 cm^{-1} due to Rh_x–CO, and a weak one at 1860 cm^{-1} due to bridge-bonded CO. After a long contact time with CO at 300 K the twin band due to gem-dicarbonyl slowly develops, which is indicative of the disruption of the Rh–Rh bonds and the formation of Rh^I sites.

2. NO Adsorption

The adsorption of NO on highly reduced Rh/Al_2O_3 has not been investigated previously. As can be seen in the spectra in Fig. 2, at low coverages a single peak appeared at 1650 cm^{-1}. With an increase in the NO exposure, bands appeared at 1660, 1722, 1822, and 1882 cm^{-1}. The intensities of the latter three bands gradually grew and shifted to higher frequencies as NO pressure was increased, with a concomitant loss in the intensity of the band at 1660 cm^{-1}. Their final positions were at 1925, 1835, and 1740 cm^{-1}.

When the temperature of Rh/Al_2O_3 reduction was lower (R_T = 873 K), similar changes were observed; the bands appeared initially at somewhat higher frequencies, and after 2 h in 40 Torr of NO they were located at 1926, 1836, and 1740 cm^{-1}. Only slight spectral changes occurred when the sample was reduced at 573 K (band maxima in this case were at 1936, 1832, and 1742 cm^{-1}) or at 1273 K (bands were at 1920, 1822, and 1728 cm^{-1}).

3. NO + CO Coadsorption

When a NO + CO gas mixture (NO/CO = 0.5) was coadsorbed on the reduced sample, intense CO bands appeared at 2107 and 2040 cm^{-1}, and broad NO bands at 1650 and 1760 cm^{-1} (Fig. 3). A weak shoulder was also observed at 2060 cm^{-1}. It is important to mention that the intensity of the band at 2107 cm^{-1} was almost twice that of the band at 2040 cm^{-1}. After an extended adsorption time, the only spectral changes were slight shifts of the bands to lower fre-

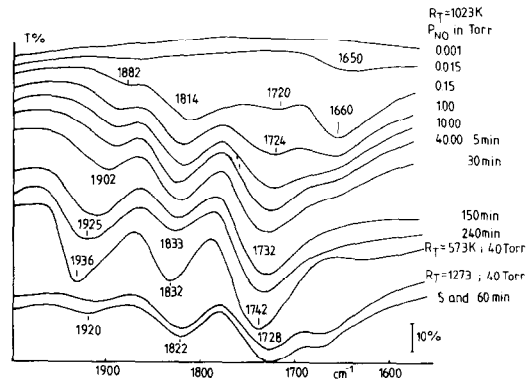

FIG. 2. Changes in the IR spectrum of 2% Rh/Al_2O_3 (R_T = 573–1273 K) at 300 K as a function of NO pressure and adsorption time.

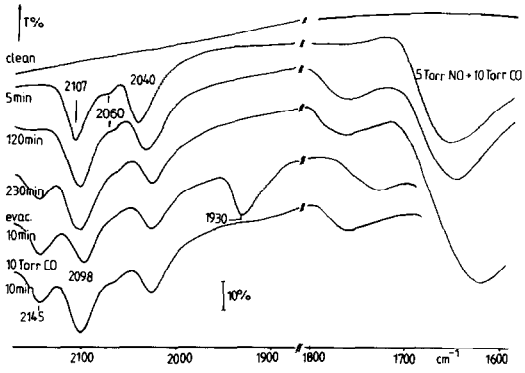

FIG. 3. Changes in the IR spectrum of 2% Rh/Al_2O_3 (R_T = 1273 K) in the presence of 5 Torr NO + 10 Torr CO gas mixture at 300 K as a function of adsorption time.

quencies and the development of a band at 2145 cm^{-1}. Evacuation of the cell at 300 K for 10 min caused an attenuation of the 2107-cm^{-1} band (as a result, the intensities of both CO bands became practically equal), shifts of the 2107- and 1760-cm^{-1} bands to 2098 and 1730 cm^{-1}, and the development of a strong band at 1930 cm^{-1}. However, no change occurred in the position and intensity of the 2145-cm^{-1} band which was the most stable absorption band; it was eliminated only above 673 K. When 10 Torr of CO was admitted into the cell, the spectrum observed before evacuation was fully restored (Fig. 3).

From a comparison of the spectra in Figs. 1 and 3, it is clear that the presence of 5 Torr of NO exerted a dramatic influence on the interaction of CO with supported Rh, which occurred very rapidly at 300 K. In order to follow this influence with time the partial pressure of NO was reduced. As can be seen in Fig. 4, in the presence of an extremely small amount of NO (0.001 Torr) the same spectra as those in the absence of NO were obtained. However, the addition of only 0.01 Torr of NO to CO (NO : CO ratio 1 : 1000) influenced the spectral changes observed in Fig. 1. In this case, the band around 2060 cm^{-1} (Rh_x–CO) remained the dominant spectral feature, but weak bands at 2100 and 2030 cm^{-1}, indicative of the formation of gem-dicarbonyl, developed at early stages of the adsorption and their intensities slowly increased in time. This behavior was more pronounced at 0.1 and 1 Torr of NO. Weak absorption bands due to adsorbed NO were detected in the presence of 1 Torr of NO.

In the next experiment, the interaction between preadsorbed CO and gaseous NO was examined. In this case, the gaseous CO was pumped off after an adsorption time of 10 min, which was not sufficient to produce any detectable gem-dicarbonyl. The spectrum of the evacuated sample showed only an intense band at 2055 cm^{-1} (Rh_x–CO) and a weak one at 1860 cm^{-1} (Rh_2–CO) (Fig. 5). These bands were completely eliminated when 5 Torr of NO was introduced into the cell. Absorption bands due to adsorbed NO appeared at 1910, 1812, 1710, and 1670 cm^{-1}. No observable spectral changes occurred in 1 h or after evacuation for 10 min. However, when the NO-covered surface was exposed to 10 Torr of CO, approximately equal intense bands were produced at 2098 and 2028 cm^{-1}, which are in all probability due to the $Rh^I(CO)$ species. The

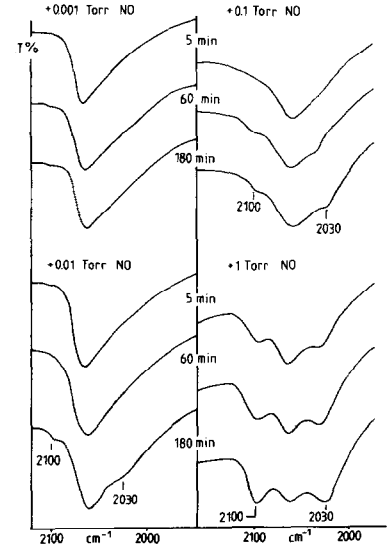

FIG. 4. Effects of the partial pressure of NO on spectral changes observed in the presence of 10 Torr CO for 2% Rh/Al_2O_3 (R_T = 1273 K) at 300 K.

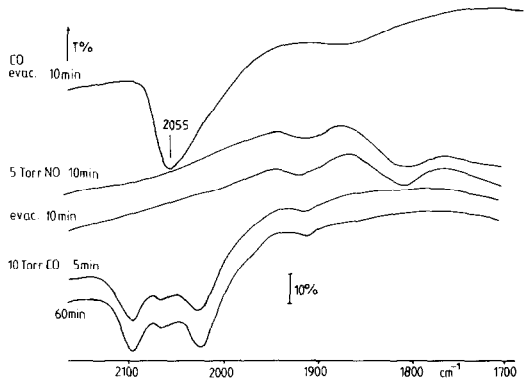

FIG. 5. Spectral changes following the interaction of adsorbed CO (NO) with NO (CO) on 2% Rh/Al_2O_3 (R_T = 1273 K) at 300 K.

presence of Rh_x–CO was also indicated by a well-resolved band at 2065 cm^{-1} (Fig. 5), which was seen even after 5 h.

The drastic effect of the NO on the CO-induced structural changes of supported rhodium was also detected at higher temperatures. As was shown previously (*11*), at and above 448 K the CO promoted the reformation of Rh_x crystallites from Rh^I sites. This was exhibited by the transformation of the gem-dicarbonyl bands into a band at 2050–2065 cm^{-1} due to Rh_x–CO. In the presence of NO this process was greatly hindered, as gem-dicarbonyl bands remained the dominant CO bands even at 523 K and their transformation occurred only after the consumption of the NO in the NO + CO reaction (Fig. 6). This is in accord with *in situ* infrared spectroscopic results obtained in the study of the NO + CO reaction in flow system (*30*).

4. O_2 + CO Adsorption

The effect of oxygen on the interaction of CO with supported Rh has been the subject of several studies (*2*). The general feature was that the previous oxidation of Rh_x or the presence of O_2 in the CO greatly enhanced the intensity of gem-dicarbonyl.

In all these cases, however, the temperature of reduction of the Rh samples was not very high (maximum 973 K) and the size of the Rh crystallites was undoubtedly much less than that in the present case. In order to facilitate explanation of the influence of NO, it seemed worthwhile to examine the effect of oxygen on the adsorption of CO on the larger Rh crystallites used in the present study.

As can be seen in Fig. 7A, the coadsorption of an O_2 + CO (1 : 2) mixture on 2% Rh/Al_2O_3 (R_T = 1273 K) led to the immediate formation of strong twin bands at 2100 and 2030 cm^{-1}, with a significantly higher intensity than that observed following the coadsorption of NO + CO mixture on the same sample. However, the disruption of Rh_x was not complete even in 2 h, as indicated by the presence of bands due to Rh_x–CO (2065-cm^{-1}) and Rh_2–CO (1860-cm^{-1}) species. Similar spectra were obtained when CO was admitted to the sample treated with 5 Torr of O_2 for 10 min at 400 K (Fig. 7B, a–c). However, exposure of the CO-covered surface (the spectrum of which exhibited a very intensed CO band at 2058 cm^{-1}) to 5 Torr of O_2 at once eliminated the CO linearly bonded to Rh_x, but left

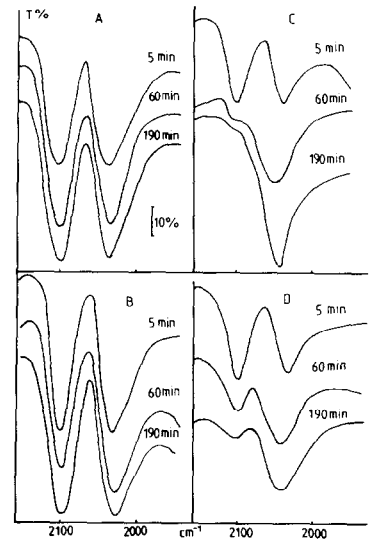

FIG. 6. Changes in the IR spectrum of 2% Rh/Al_2O_3 (R_T = 573 K) in the presence of 5 Torr of NO and 10 Torr of CO at (A) 423 K, (B) 473 K, and (C) 523 K as a function of adsorption time. (D) In the absence of NO at 473 K.

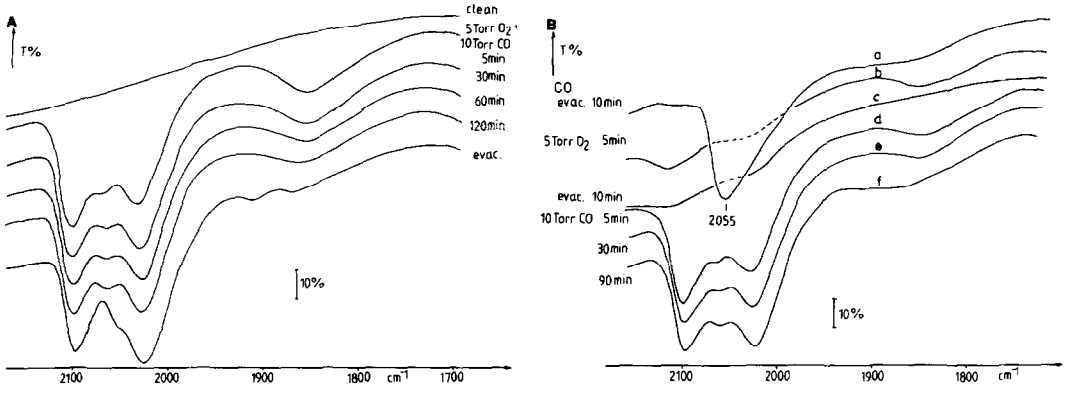

FIG. 7. (A) Changes in the IR spectrum of 2% Rh/Al_2O_3 (R_T = 1273 K) in the presence of 5 Torr O_2 + 10 Torr CO at 300 K as a function of adsorption time. (B) Spectral changes following the interaction of adsorbed CO (O) with O_2 (CO) on the same sample at 300 K.

the weak bridged CO unchanged (Fig. 7B, d–f). A weak band was seen at 2115 cm^{-1} which is very probably due to the $Rh\begin{matrix}CO\\O\end{matrix}$ species.

DISCUSSION

The presence of NO exerted a dramatic influence on the development of gem-dicarbonyl, which is indicative of the occurrence of oxidative disruption of the Rh_x crystallites. The interpretation of this effect and the spectral changes observed in the NO–CO interaction requires a brief survey of the characteristic features of the interaction of NO with Rh, as established by means of vibrational spectroscopy.

1. Adsorption of NO on Rh

The adsorption of NO on highly dispersed Rh supported on alumina produced four absorption bands at 300 K; these were assigned to $Rh–NO^+$ (1920 cm^{-1}), Rh–NO (1838 cm^{-1}), and $Rh–NO^-$ (1740 and 1660 cm^{-1}) (*20, 21*). Initially, the intensity of the band at 1920 cm^{-1} was small, but it was enhanced after prolonged adsorption at 300 K or after high-temperature treatment of the sample with NO, which was accompanied by intensity decreases for other NO bands. This feature strongly suggested that the 1920-cm^{-1} band is associated with the partial oxidation of Rh_x or with the presence of adsorbed oxygen (*21*). The subsequent work on this system confirmed the positions of the NO bands and their basic behavior (*28–30*). Somewhat different positions of the NO bands were observed for RhY zeolite which contained Rh^I in high concentrations, as the sample had not been reduced after preparation, but only evacuated at 250–350 K (*31*). The intense bands at 1780 and 1860 cm^{-1} were assigned to the symmetric and asymmetric stretches of the dinitrosyl species, $Rh(NO)_2$; this assignment was supported by the results of isotopic labeling. Formation of the dinitrosyl complex has been assumed to occur on a reduced Rh/Al_2O_3 sample, too; the 1743- and 1825-cm^{-1} bands were attributed to this species (*28*). Their invariant ratio with coverage change and the isotopic data obtained by Liang *et al.* (*29*) were in harmony with this assumption. Adsorption data on the $NO–Rh/Al_2O_3$ system also indicated that NO undergoes multiple adsorption on highly dispersed Rh (*32*). On the other hand, Dictor (*30*) accepted the original assignments of the above bands (*20, 21*), as he found that the ratios of the two bands varied in different ways under various conditions.

New features of the adsorption of NO on

Rh emerged from recent EELS studies on single-crystal surfaces at low temperatures, ~85–95 K (*33–36*). On the Rh(331) surface, a strong loss was observed at 1705 cm^{-1} and a very weak one at 1815 cm^{-1} (*33*). On Rh(111) a twofold bridge-bonded NO was established, the band of which shifted from 1480 to 1630 cm^{-1} as the coverage increased (*34*). At higher coverages, another small loss peak was observed at 1840 cm^{-1}, which did not shift appreciably with coverage change. This loss was ascribed to terminal NO adjacent to traces of coadsorbed oxygen (*34*). Preadsorbed oxygen significantly increased the relative intensity of the 1840-cm^{-1} loss and induced the formation of a weak loss peak at 1755 cm^{-1} (*35*). On Rh(100), two vibrational modes of adsorbed NO were detected at 895 and 1580 cm^{-1} and were assigned to a lying-down or highly inclined species and a vertically adsorbed species (*36*). The former was favored at low coverages, but not at more crowded higher coverage surfaces.

2. *Disruption of Rh_x Crystallites*

In the explanation of the effect of NO we can assume that NO participates directly in the CO-induced disruption of Rh_x crystallites or, independently of this process, the adsorption of NO can also disrupt the Rh–Rh bonds, leading to isolated Rh^0 atoms, or through oxidation, to Rh^I sites on which CO binds in the twin form. As the binding energy of NO to a Rh_x cluster is higher than that for CO (*20, 21, 34*), the driving force assumed to be decisive in the disruption of the Rh–Rh bonds (i.e., the formation of a strong adsorbate–Rh bond (*8, 11*)) will be greater than that for CO adsorption. By the same argument, the products of dissociation of NO on Rh_x (adsorbed nitrogen and oxygen), which form very strong bonds with Rh_x, could also contribute to the disruption of Rh_x crystals. Our recent measurements showed that at least 25% of the NO adsorbed at saturation dissociates on a Rh(111) sample under UHV conditions at 300 K (*37*), and there are strong indications that a similar process also occurs on supported Rh (*20, 21, 38*). Accordingly, we can assume the occurrence of the sequence of the following reactions, which produce smaller Rh clusters and finally atomically dispersed Rh atoms,

$$Rh_x + NO_{(g)} = Rh_x\text{–}NO$$

$$Rh_x\text{–}NO + NO_{(g)} = Rh_{x-y}\text{–}NO + Rh_y^0\text{–}NO \quad (y < x)$$

$$2Rh_y\text{–}NO = Rh_{2y-1}\text{–}NO + Rh^0\text{–}NO$$

$$Rh_x\text{–}NO = Rh_{x-y}\text{–}N + Rh_y\text{–}O$$

(Rh^0 is atomically dispersed Rh).

The atomically dispersed Rh is easily oxidized by adsorbed oxygen, hydroxyl, and nitric oxide to yield Rh^I sites,

$$Rh_y\text{–}NO = Rh_{y-1} + Rh^+ + NO^-$$

$$Rh_y\text{–}NO = Rh_{y-2} + 2Rh^+ + O^{2-} + \tfrac{1}{2}N_2$$

$$Rh_y\text{–}O = Rh_{y-1} + Rh^+ + O^-$$

$$Rh^0 + OH^- \text{ (support)} = Rh^+ + O^{2-} + \tfrac{1}{2}H_2.$$

If the above processes occur in the interaction between NO and Rh_x, they should be exhibited in spectral changes following NO adsorption on the Rh sample, assuming that the NO adsorbed on Rh clusters and that on Rh^I, sites are characterized by different absorption bands.

As demonstrated in Fig. 2, spectral changes (although not as dramatic as those for CO adsorption) do occur in the course of the interaction of NO with Rh_x crystallites at 300 K. They comprise the gradual formation of a pair of bands at 1740 and 1836 cm^{-1}, and the development of a band at 1934 cm^{-1}.

Taking into account the characteristic vibration of dinitrosyl on Rh^I supported on Y-zeolite (*31*), one can tentatively assign the 1740- and 1830-cm^{-1} bands to the symmetric and asymmetric stetches of the $Rh^I(NO)_2$ species. As the reduced sample (R_T = 773–1273 K) initially contains neither

isolated Rh atoms nor Rh^I sites (*8, 11*), the development of these bands can be considered to be a result of the oxidative disruption of Rh_x by NO. We may expect that Rh^I sites are generated more rapidly for the highly dispersed system (R_T = 573 K) than for the less dispersed system (R_T = 773–1273 K). In harmony with this consideration, the intensity of the pair of bands at 1720–1740 and 1810–1836 cm^{-1} was higher for the sample reduced at lower temperatures, and they appeared at higher frequencies, even at the beginning of the adsorption, than those for the sample with R_T = 1023 K (Fig. 2). In the latter case, a considerably longer contact time was required to attain this state. Since neither of these bands was identified by means of EELS on clean Rh single-crystal surfaces at ~90 K, but they did develop when the surface contained traces of adsorbed oxygen or when NO dissociated (*34, 35*), it seems likely that the formation of the bands at 1720–1740 and 1810–1830 cm^{-1} is associated with a partial oxidation of the supported Rh.

The fact that, even after an extended adsorption time, and starting with highly dispersed Rh (R_T = 573 K), we could not reach the positions of the bands (1780 and 1860 cm^{-1}) reported by Iizuka and Lunsford (*31*) for the NO–Rh^I zeolite system may mean that the transformation of Rh_x to Rh^I was not complete in either case (*20, 21, 27, 28–30*) or, more probably, the sample of Iizuka and Lunsford contained Rh^{3+} ions. Consequently, the absorption bands of dinitrosyl appeared at higher frequencies.

The observation that the gem-dicarbonyl band became the dominant one in the spectrum following NO–CO coadsorption on Rh_x aggregates suggests that the disruption of a certain portion of the Rh_x was quite fast also on this sample. Rh^I was formed in a significant concentration, and CO binds to this more strongly than NO.

3. *Reductive Agglomeration of Rh^I Sites*

As was mentioned in the Introduction, at higher temperatures, from 448 K, the effect of CO on the topology of supported Rh is different. In this case it promotes the transformation of the gem-dicarbonyl, $Rh^I(CO)_2$, into Rh_x–CO species, i.e., the reductive agglomeration of Rh^I to Rh_x crystallites. This process was characterized by the equation (*18*)

$$2Rh^I(CO)_2 + O^{2-} = Rh_x\text{–}CO + CO_2 + 2CO \quad (x = 2).$$

As was demonstrated in Fig. 6, in the presence of NO this process was greatly hindered; absorption bands due to $Rh^I(CO)_2$ were the dominant bands even at 523 K, which means that the NO exerts a great stabilizing influence on the Rh^I sites, very probably owing to its oxidizing properties.

4. *Formation of Other Surface Species*

There are several spectral features which indicate that, in the presence of a NO + CO gas mixture, another surface species, e.g., $Rh\begin{smallmatrix}CO\\NO\end{smallmatrix}$, also forms on the surface. These features are as follows: (i) the intensity of the high-frequency (HF) band of gem-dicarbonyl is higher than that of the low-frequency (LF) band; (ii) the HF band appears at a slightly higher frequency (2107 cm^{-1}) than that corresponding to the symmetric stretch of $Rh^I(CO)_2$; (iii) there is also a shift in the position of the NO band (from 1740 to 1760 cm^{-1}) in the presence of CO.

These characteristics were considered evidence of the formation of the $Rh\begin{smallmatrix}CO\\NO\end{smallmatrix}$ complex, where the 2107-cm^{-1} band was attributed to ν_{CO} and the 1760-cm^{-1} band to ν_{NO} for this species (*20, 21*). The formation of this species on supported Rh was also established by Hyde *et al.* (*28*), although it was not identified in the high-temperature (above 473 K) interaction of NO + CO (*30*). However, it is still an open question whether this fraternal twin complex forms

on Rh crystallites or on Rh^I sites. The results of the present work provide no evidence for the existence of this complex on Rh_x crystallites. In this case we should have observed the reaction of the interaction of Rh_x–CO with NO,

$$Rh_x\text{–}CO + NO_{(g)} = Rh_x\begin{matrix}CO\\NO\end{matrix}$$

but instead the complete replacement of the adsorbed CO occurred (Fig. 5):

$$Rh_x\text{–}CO + NO = Rh_x\text{–}NO + CO_{(g)}$$

On the other hand, the replacement of one CO in gem-dicarbonyl

$$Rh^I\begin{matrix}CO\\CO\end{matrix} + NO_{(g)} = Rh^I\begin{matrix}CO\\NO\end{matrix} + CO_{(g)}$$

occurred rapidly, yielding the characteristic bands at 2107 and ~1760 cm^{-1}. Therefore, we incline to the view that the Rh^I sites are the adsorption sites for formation of the $Rh^I\begin{matrix}CO\\NO\end{matrix}$ complex, and its production on the present sample is strongly connected with the occurrence of the oxidative disruption of the aggregates and with the formation of Rh^I sites. We note here that a fraternal twin species has also been detected by means of infrared spectroscopy on a Pd/zeolite sample (*39, 40*), and ESR measurements led to its being ascribed to Pd^{II} centers (*39*).

Following degassing of the sample at 300 K, the intensities of the 2100- and 2030-cm^{-1} bands became almost equal (Fig. 3), the NO band at 1760 cm^{-1} disappeared and the band at 1930 cm^{-1} (absent in the presence of a NO + CO gas mixture) appeared; these findings indicate that the fraternal twin species decomposes during evacuation, according to the reaction

$$Rh^I\begin{matrix}CO\\NO\end{matrix} = Rh^I\text{–}NO + CO_{(g)}$$

The fraternal structure can be reestablished by introducing CO into the cell (Fig. 3), but never by NO admission, which proves that the CO and not the NO desorbed in its decomposition. The spectral changes observed confirm our previous conclusion that the $Rh^I\begin{matrix}CO\\NO\end{matrix}$ complex is more unstable than the $Rh^I\begin{matrix}CO\\CO\end{matrix}$ species (*21*). Therefore, it is not surprising that Dictor (*30*) could not identify it at 473 K.

After an extended adsorption time of NO + CO gas mixture a relatively strong band also developed at 2145 cm^{-1} (Fig. 3). The formation of this band required the presence of a more significant amount of NO, as it was not detected at lower NO pressures (Fig. 4). This band was also identified by means of infrared spectroscopy in the high-temperature reaction of NO + CO on highly dispersed Rh (*26, 30, 41*), while it was missing from the spectra reported by other workers (*20–22, 27, 28*). The formation of a similar band occurred in the NO + CO reaction for Cr_2O_3/Al_2O_3 catalyst which was assigned to adsorbed cyanide ion on the basis of isotope experiments (*42*). A similar assignment was proposed for the 2145-cm^{-1} band formed on Rh/Al_2O_3 (*26, 30, 41*), which, taking into account the location and stability of this band, seems very reasonable. The cyanide species on Rh was found to be a very stable species; its desorption occurred only above 500 K (*43*).

A priori, another candidate for the 2145-cm^{-1} band would be an isocyanate species. However, the asymmetric stretch of NCO on Rh appears in a higher frequency region, 2170–2190 cm^{-1} (*21, 23*), and in addition, the NCO species decomposed at 300–350 K on both supported Rh (*44*) and Rh single-crystal surfaces (*45*). Further investigations concerning the mechanism of cyanide formation in the NO + CO surface interaction are clearly required.

5. Effect of Oxygen

It was demonstrated that oxygen can also promote the formation of gem-dicarbonyl, which is a well-known feature. However, it should be pointed out that in the previous cases the effect of oxygen was examined in the case of highly dispersed Rh (low reduction temperature), on which the adsorption of CO (even in the absence of oxygen) results in the formation of gem-dicarbonyl. In the present case, the dominant band following CO adsorption was that of linearly bonded CO, Rh_x–CO, and even after adsorption for 60 min there was no indication of the formation of gem-dicarbonyl. For the production of this species, it was sufficient to bring the Rh_x cluster in contact with oxygen at 300 K. This suggests that the adsorption of oxygen on Rh_x at 300 K induces a fast oxidative disruption of Rh_x aggregates as discussed earlier.

Due to the strong adsorption of oxygen on Rh_x, oxygen does not convert the CO bonded in the form of Rh_x–CO to the twin species, $Rh^{I}(CO)_2$, in the absence of gaseous CO. Instead, the adsorbed CO is first replaced by oxygen:

$$Rh_x\text{–}CO + \tfrac{1}{2}O_{2(g)} = Rh_x\text{–}O + CO_{(g)}$$

It appears that the amount of CO desorbed in this process is small enough for appreciable spectral changes to be produced (e.g., production of bands due to $Rh^{I}(CO)_2$) after readsorption on Rh^{I} sites formed in the oxygen-induced disruption processes.

REFERENCES

1. Yang, A. C., and Garland, C. W., *J. Phys. Chem.* **61,** 1504 (1957).
2. Worley, S. D., Rice, C. A., Mattson, G. A., Curtis, C. W., Guin, J. A., and Tarrer, A. R., *J. Chem. Phys.* **76,** 20 (1982), and references therein.
3. Yates, J. T., Jr., Duncan, T. M., and Vaughan, R. W., *J. Chem. Phys.* **71,** 3908 (1979).
4. Yates, J. T., Jr., Duncan, T. M., Worley, S. D., and Vaughan, R. W., *J. Chem. Phys.* **70,** 1219 (1979).
5. Yates, D. J. C., Murrell, L. L., and Prestridge, E. B., *J. Catal.* **57,** 41 (1979).
6. Primet, M., *J. Chem. Soc. Faraday Trans. 1* **74,** 2570 (1978).
7. Primet, M., Védrine, J. C., and Naccache, G., *J. Mol. Catal.* **4,** 411 (1978).
8. van 't Blik, H. F. J., van Zon, J. B. A. D., Huizinga, T., Vis, J. C., Koningsberger, D. C., and Prins, R., *J. Phys. Chem.* **87,** 2264 (1983).
9. van 't Blik, H. F. J., van Zon, J. B. A. D., Koningsberger, D. C., Prins, R., *J. Mol. Catal.* **25,** 379 (1984).
10. van 't Blik, H. F. J., van Zon, J. B. A. D., Huizinga, B., Vis, J. C., Koningsberger, D. C., and Prins, R., *J. Amer. Chem. Soc.* **107,** 3139 (1985).
11. Solymosi, F., and Pásztor, M., *J. Phys. Chem.* **89,** 4789 (1985).
12. Smith, A. K., Hughes, F., Theolier, A., Basset, J. M., Ugo, R., Zanderighi, G. M., Bilhou, J. L., Bilhou-Bougnol, V., and Graydon, W. F., *Inorg. Chem.* **18,** 3104 (1979).
13. Bergeret, G., Gallezot, P., Gelin, P., Ben Taarit, Y., Lefebvre, F., Naccache, C., and Shannon, R. D., *J. Catal.* **104,** 279 (1987).
14. Solymosi, F., and Erdöhelyi, A., *Surf. Sci.* **110,** L630 (1981).
15. Erdöhelyi, A., and Solymosi, F., *J. Catal.* **84,** 446 (1983).
16. Zaki, M. J., Kunzmann, G., Gates, B. C., and H. Knözinger, *J. Phys.Chem.* **91,** 1486 (1987).
17. Basu, P., Panayotov, D., and Yates, J. T., Jr., *J. Phys. Chem.* **91,** 3133 (1987).
18. Solymosi, F., and Pásztor, M., *J. Phys. Chem.* **90,** 5312 (1986).
19. Solymosi, F., and Pásztor, M., *J. Catal.* **104,** 312 (1987).
20. Arai, H., and Tominaga, H., *J. Catal.* **43,** 131 (1976).
21. Solymosi, F., and Sárkány, J., *Appl. Surf. Sci.* **3,** 68 (1979).
22. Unland, M. L., *J. Catal.* **31,** 459 (1973).
23. Lorimer, D'A., and Bell, A. T., *J. Catal.* **59,** 223 (1979).
24. Solymosi, F., and Bánsági, T., *J. Phys. Chem.* **83,** 552 (1979).
25. Raskó, J., and Solymosi, F., *J. Catal.* **71,** 219 (1981).
26. Solymosi, F., Völgyesi, L., and Raskó, J., *Z. Phys. Chem. N.F.* **120,** 79 (1980).
27. Hecker, W. C., and Bell, A. T., *J. Catal.* **85,** 389 (1984).
28. Hyde, F. A., Rudham, R., and Rochester, C. H., *J. Chem. Soc. Faraday Trans. 1* **80,** 531 (1984).
29. Liang, J., Wang, H. P., and Spicer, L. D., *J. Phys. Chem.* **89,** 5840 (1985).
30. Dictor, R., *J. Catal.* **109,** 89 (1988).
31. Iizuka, T., and Lunsford, J. H., *J. Mol. Catal.* **8,** 391 (1980).

32. Yao, H. C., Japar, S., and Shelef, M., *J. Catal.* **50,** 407 (1977).

33. Dubois, L. H., Hansma, P. K., and Somorjai, G. A., *J. Catal.* **65,** 318 (1980).

34. Root, T. W., Fisher, G. B., and Schmidt, L. D., *J. Chem. Phys.* **85,** 4679 (1986).

35. Root, T. W., Fisher, G. B., and Schmidt, L. D., *J. Chem. Phys.* **85,** 4687 (1986).

36. Villarubia, J. S., and Ho, W., *J. Chem. Phys.* **87,** 750 (1987).

37. Solymosi, F., Bugyi, L., and Kiss, J., *Surf. Sci.* **188,** 475 (1987).

38. Chin, A. A., and Bell, A. T., *J. Phys. Chem.* **87,** 3700 (1983).

39. Che, M., Dutel, J. P., Gallezot, P., and Primet, M., *J. Phys. Chem.* **80,** 2371 (1976).

40. Raskó, J., and Solymosi, F., *J. Chem. Soc. Faraday Trans. 1* **80,** 1841 (1984).

41. Solymosi, F., and Novák, É., submitted for publication.

42. Raskó, J., and Solymosi, F., *J. Chem. Soc. Faraday Trans. 1* **76,** 2383 (1980).

43. Solymosi, F., and Bugyi, L., *Surf. Sci.* **147,** 685 (1984).

44. Solymosi, F., Raskó, J., and Bánsági, T., "Proc. Intern. Symp. on Spillover of Adsorbed Species" (G. M. Pajonk, S. J. Teichner, and J. E. Germain, Eds.), p. 109. Elsevier, Amsterdam, 1983.

45. Solymosi, F., and Kiss, J., *Surf. Sci.* **134,** 243 (1983).